



In vitro studies of biofilm-forming *Bacillus* strains, biocontrol agents isolated from the maize phyllosphere

Aluminé Fessia^{a,d,*}, Melina Sartori^{a,d}, Daiana García^{a,d}, Luciana Fernández^{b,c,d},
Rodrigo Ponzio^{b,c,d}, Germán Barros^{a,d}, Andrea Nesci^{a,d}

^a Laboratorio de Ecología Microbiana, Departamento de Microbiología e Inmunología, Facultad de Ciencias Exactas, Físico-Químicas y Naturales, Universidad Nacional de Río Cuarto, Ruta Nacional 36, Km 601, X5804ZAB, Río Cuarto, Córdoba, Argentina

^b Departamento de Física, Departamento de Química, Facultad de Ciencias Exactas, Físico-Químicas y Naturales, Universidad Nacional de Río Cuarto, CONICET, X5804BYA, Río Cuarto, Argentina

^c Instituto de Investigaciones en Tecnologías Energéticas y Materiales Avanzados (IITEMA), Universidad Nacional de Río Cuarto, Ruta Nacional 36, Km 601, X5804ZAB, Río Cuarto, Córdoba, Argentina

^d Consejo Nacional de Investigaciones Científicas y Técnicas (CONICET), Argentina

ARTICLE INFO

Keywords:

Biofilm
Bacillus
Environmental conditions
Motility
Phyllosphere

ABSTRACT

We aimed to assess how biofilm formation by three *Bacillus* isolates was affected by changes in temperature, water potential, growth media, time, and the combinations between these factors. The strains had been selected as potential biological control agents (BCAs) in earlier studies, and they were identified as *B. subtilis* and *B. velezensis* spp. through 16 rRNA sequencing and MALDI-TOF MS. Maize leaves (ML) were used as one of the growth media, since they made it possible to simulate the nutrient content in the maize phyllosphere, from which the bacteria were originally isolated. The strains were able to form biofilm both in ML and biofilm-inducing MSgg after 24, 48, and 72 h. Biofilm development in the form of pellicles and architecturally complex colonies varied morphologically from one strain to another and depended on the conditions mentioned above. In all cases, colonies and pellicles were less complex when both temperature and water potential were lower. Scanning electron microscopy (SEM) revealed that changing levels of complexity in pellicles were correlated with those in colonies. Statistical analyses found that the quantification of biofilm produced by the isolates was influenced by all the conditions tested. In terms of motility (which may contribute to biofilm formation), swimming and swarming were possible for all strains in 0.3 and 0.7% agar, respectively. A more in-depth understanding of how abiotic factors influence biofilm formation can contribute to a more effective use of these biocontrol strains against pathogens in the maize phyllosphere.

1. Introduction

Bacteria can live in biofilms, which are organized communities of aggregated cells embedded in a self-produced extracellular polymeric matrix (EPS) [1]. In fact, more than 99% of all bacteria exist in this form [2]. More than half of the total bacterial population on parsley, endives, and alfalfa sprouts has been observed to live in biofilms [3–5]. More generally, 70% of the bacteria on leaves have this lifestyle [6]. The structural complexity of biofilms enhances bacterial survival, adaptation and dissemination in natural, industrial and medical systems [7]. Biofilms can help the cells of both harmful and potentially beneficial bacteria to become attached to the leaf surface and colonize it, as well as

offer protection against adverse conditions [6,8].

The phyllosphere is a complex above-ground ecosystem where specific but dynamic interactions take place between the host plant and the existing microbial communities. These communities should be adapted to fluctuating conditions regarding temperature, light, UV radiation, and water and nutrient availability [9]. Their composition and diversity vary depending on such environmental elements, as well as on plant species, leaf age, and the co-existence with other pathogenic and non-pathogenic microorganisms [10,11]. They may inhabit the leaf's external and internal surfaces, i.e. they may be either epiphytes or endophytes. Many of them play an important role in protecting the plant against foliar diseases or in limiting adverse effects on plant health and

* Corresponding author. Laboratorio de Ecología Microbiana, Departamento de Microbiología e Inmunología, Facultad de Ciencias Exactas, Físico-Químicas y Naturales, Universidad Nacional de Río Cuarto, Ruta Nacional 36, Km 601, X5804ZAB, Río Cuarto, Córdoba, Argentina.

E-mail address: afessia@exa.unrc.edu.ar (A. Fessia).

<https://doi.org/10.1016/j.biofilm.2022.100097>

Received 9 August 2022; Received in revised form 8 November 2022; Accepted 18 November 2022

Available online 5 December 2022

2590-2075/© 2022 The Authors. Published by Elsevier B.V. This is an open access article under the CC BY-NC-ND license (<http://creativecommons.org/licenses/by-nc-nd/4.0/>).

productivity [12]. They are able to do so thanks to their intimate associations with the leaves, their adaptability, and the fact that they share the same niche as the pathogens, which typically undergo an epiphytic phase before entering the plant cell or the apoplast (intercellular space) [13]. For this reason, a fast-growing field of research focuses on microorganisms with the ability to biocontrol such diseases, as is the case of the remarkably popular *Bacillus* species [14].

As part of biocontrol strategies, therefore, leaves may be inoculated with epiphytic microorganisms isolated from the same ecosystem as the foliar pathogens they are supposed to antagonize. The ability of these microorganisms to form aggregates and produce signaling compounds enables them to become attached to the leaf surface and create biofilm, which in turn makes them more likely to successfully inhibit pathogens [5]. This is why biocontrol schemes in agriculture could benefit from more in-depth knowledge about biofilm's involvement in the interactions between biocontrol agents and pathogens, in terms of competition for space and nutrients, tolerance/resistance, and physiology [15,16]. Several studies have looked into how biofilm formation changes depending on the bacterial strain and factors such as temperature, pH, nutrient availability, minerals, the flow of fluids, plant defense compounds, and surfactants [17]. For example, the combination of low or high temperature with an optimum or reduced water regime systematically influences the interaction between *Bacillus amyloliquefaciens* strain S499 and the plants it colonizes [18].

Maize (*Zea mays* L.) is one of the main crops grown in Argentina, with an average annual production of 54 million tons and a planting area of 7.7 million ha [19]. It is commonly affected by the endemic disease known as Northern corn leaf blight (NCLB), caused by foliar pathogen *Exserohilum turcicum* (Pass.) Leonard and Suggs (Syn. *Helminthosporium turcicum* Pass.) [20]. In a previous study, we selected microbial isolates from the maize phyllosphere, on the basis of their ability to compete against *E. turcicum* and alter its growth parameters. This ability was measured through a dominance index. At water potential values (Ψ) of -1.38 MPa and -4.19 MPa, three *Bacillus* isolates were dominant at a distance (5/0) and significantly reduced the pathogen's growth rate *in vitro* by between 84 and 98% [21]. A second *in planta* study in the greenhouse started out with 11 *Bacillus* isolates, and the same three as before showed potential as biological control agents against *E. turcicum* [22]. Since the real efficiency of an agent of this kind can only be confirmed on the field, another study [23] measured the incidence of NCLB and common rust on a maize field, after applying the antagonists selected *in vitro* and *in planta*. In agreement with the earlier observations, the incidence of both diseases was significantly reduced. In the case of NCLB, incidence was over 50% lower after 40 days of initial inoculation with the *Bacillus* spp.

Later, eight isolates from the maize phyllosphere, including the three *Bacillus* strains from the previous assays, were analyzed for their modes of action and their tolerance to different environmental conditions. Their antagonistic potential differed according to their mode of action (enzymatic activity, the production of volatile organic compounds, and/or direct antibiosis through other secondary metabolites). In addition, they were tolerant to changes in UV radiation, temperature, and osmotic stress, and thus more likely to survive on the leaf surface [24].

Although the ubiquity of biofilm probably means that it is critical for bacterial persistence in a given ecosystem, very few studies have considered its role in agriculture and particularly in the ecology of potential biocontrol agents in the maize phyllosphere. This is a key piece of information when designing preventive biocontrol strategies. For this reason, the present study assessed the ability of the three previously selected *Bacillus* isolates to form biofilm under varying conditions. More specifically, our aims were: (a) to complete the identification of the isolates; (b) to determine their ability to form biofilms *in vitro*; (c) to investigate the effects of temperature, water potential, growth media and time on this ability; and (d) to evaluate the isolates' motility under different conditions.

2. Methods

2.1. Identification of biological control agents (BCAs)

The three *Bacillus* spp. isolates used in this study were taken from the leaves of maize grown in the province of Córdoba, Argentina. They had been previously selected as potential biological control agents (BCAs) against *E. turcicum* [21–24]. Their identification at the genus level [21] followed Bergey's Manual of Systematic Bacteriology [25]. Further identification was achieved on the basis of biochemical traits using API 50 CH (bioMérieux, Lyon, France), as well as molecularly through 16S–23S RNA sequencing. Isolates EM-A7 and EM-A8 were found to be highly similar to *B. subtilis*, whereas EM-A6 could not be strongly discriminated among *Bacillus* species [24].

Matrix-assisted laser desorption/ionization-time of flight mass spectrometry (MALDI-TOF MS Bruker Daltonik®, Bremen, Germany) was performed here to complement the earlier identification studies. Ethanol formic acid was used for extraction and the assay was carried out by the Laboratorio de Bacteriología Hospital de Clínicas José de San Martín (Universidad de Buenos Aires, Argentina). A score was obtained for each isolate. Guidelines by the National Network for Microbiological Identification by Mass Spectrometry in Argentina (RENAEM) (<http://anlis.gov.ar/renaem/>) suggest there should be a minimum 10% difference between the first and the second matching species for a different species to be identified [26]. The score cut-offs recommended by the manufacturer were ≥ 2.000 for species level, 1.700 to 1.999 for genus level, and < 1.700 for non-reliable identification. The results were confirmed by 16S rRNA sequencing as the reference molecular technique. The sequences were obtained with sequencing primers 785F 5'-GGATTA GATACCCTGGTA-3' and 907R 5'-CCGTCAATTCMTTTRAGTTT-3' and PCR primers 27F 5'-AGAGTTTGA TCMTGGCTCAG-3 and 1492R 5'-TACGGYTACCTTGTTACG ACTT-3' from the sequencing service of Macrogen Inc. (Seoul, Korea). Their degree of similarity at DNA level with reported sequences was established using BLAST (Search Tools for Local Alignments, URL: <http://www.ncbi.nlm.nih.gov/BLAST/Blast.cgi>). The 16s rRNA sequencing data were registered in GenBank under accession numbers OL704803-OL704805.

The three isolates were stored at -20 °C in skim-milk medium (Tryptic soy broth, milk 20% p/v) (Britania, BA, Argentina) with the addition of 20% v/v glycerol.

2.2. Development of biofilm in the form of pellicles and architecturally complex colonies

The pellicle assays followed [27,28] with minor modifications. First, the three isolates (EM-A6, EM-A7 and EM-A8) were individually grown overnight in Nutrient Broth (NB) (5 g l^{-1} pluripeptone and 5 g l^{-1} meat extract) (Britania, BA, Argentina) at 30 °C and 140 rev min^{-1} . The cells were diluted (1:100) in 40 ml of NB and incubated at 30 °C on a rotary shaker (140 rev min^{-1}) (Model BM081, Biomint, Argentina) until reaching OD_{600} 0.3–0.5. Then, 1.5 ml of medium were placed on 24-well plates (Sorfa, Genbiotech, Argentina) and three μL of cell suspension were added (dilution 1:500). The plates were incubated at 20, 25 and 30 °C for 72 h without agitation. The medium was either biofilm-inducing MSgg medium (0.1 mol l^{-1} MOPS, 2 mM l^{-1} MgCl_2 , 0.05 mM l^{-1} MnCl_2 , $1 \mu\text{M l}^{-1}$ ZnCl_2 , $2 \mu\text{M l}^{-1}$ thiamine, $700 \mu\text{M l}^{-1}$ CaCl_2 , 50 mg l^{-1} phenylalanine, 0.5% v/v glycerol, and 0.5% p/v glutamate), or maize leaves broth (MLB). The latter was chosen because the bacteria were isolated from fresh maize leaves [21]. It was made by boiling 30 g of fresh maize leaves in 1 l of water for 60 min, and filtering the suspension through a double layer of muslin. Distilled water was added until a 1 l volume was obtained. When necessary, this medium was supplemented with 1.5% agar, which will from hereon be referred to as MLA (maize leaves agar) instead of simply MLB.

Biofilm formation was assessed in relation with the following conditions: type of medium, water potential values ($\Psi = -7.06$ MPa ($a_w = 0.95$); -4.19 MPa ($a_w = 0.97$); and -1.38 MPa ($a_w = 0.99$), and

incubation temperatures (20, 25, and 30 °C). Water activity in the media was modified with glycerol (Dallyn and Fox, 1980). In representative media samples, this activity was measured with an AquaLab meter (model 4 TE AquaLab Technologies, Riverside, CA) and converted to water potential (Ψ). Water activity (a_w) is the universally-used term for the availability of water in a solution. It is the ratio of water vapor pressure in equilibrium to that of pure water at the same temperature. The availability of water for microbial development and metabolism in environmental terms is defined as water potential (Ψ). Given the nature of our study, this is the factor that we assessed and the one we will refer to throughout this paper.

To study biofilm through the formation of colonies, the bacterial inocula were prepared in the same way as for the pellicle assay [28]. Three μL of cell suspension were symmetrically spotted on dry MSgg or MLA 1.5% p/v agar plates; more precisely, three drops were placed on each Petri dish (50 mm in diameter). The droplets were left to become absorbed before moving the plates, which were incubated at 20, 25, and 30 °C for 72 h without agitation under different environmental conditions.

The architecture of the pellicles and colonies formed by each isolate under these different conditions was observed and photographed with a stereoscopic microscope (Motic, DM-39-N9GO, Hong Kong, Asia) connected to a Motic Images Plus 2.0 digital camera. Each image is representative of triplicate assays performed in three independent experiments. *Bacillus subtilis* NCIB3610 (a wild-type reference strain) was used as a positive control [29,30], and *B. subtilis* JH642 (a domesticated, laboratory strain) was used as the negative control, since it forms flat and featureless colonies and pellicles [31].

2.3. Visualization of colony by scanning electron microscopy (SEM)

To compare and visualize biofilm structure under different conditions, biofilm samples were observed through scanning electron microscopy (SEM), according to Refs. [28,32]. Colonies were grown as described above, and fixed in a solution made up of 2.7% v/v paraformaldehyde, 1.7% v/v glutaraldehyde, and 0.1 m l^{-1} phosphate buffer (pH 7.2) at room temperature for 2 h on a rotary shaker. Subsequently, the plates were kept at 4 °C overnight, washed with PBS and incubated for 5 min at room temperature. Afterwards, the samples were dehydrated in a series of ethanol solutions from 30% v/v to 100% v/v. Five-mm samples were mounted on aluminum stubs and held with double-sided carbon tape. They were then coated with a thin layer of gold and taken for observation under a FEG-SEM microscope (Zeiss Sigma, Oberkochen, Germany). The images were obtained with an in-lens detector of secondary electrons, using 3 keV as energy.

2.4. Quantification of biofilm formation under the effects of different types of media, water potentials, and temperatures

Biofilm formation was quantified as described by Refs. [33,34] with some modifications. The influencing factors considered were the type of medium (MSgg or MLB), water potential values ($\Psi = -7.06, -4.19$ and -1.38 MPa), and incubation temperatures (20, 25 and 30 °C). Quantifications were performed at 24, 48, and 72 h. To do this, the three isolates were cultured overnight in NB medium, at 30 °C on a rotary shaker at 140 rev min^{-1} . Then, 400 μL were transferred to 40 ml of NB and incubated under the same conditions until reaching OD_{600} 0.3–0.5 (mid-exponential phase). Two μL of this dilution were transferred to 96-well microtiter plates (Corning, Croce, Argentina) containing 198 μL of either MSgg broth or MLB. The microplates were incubated at 20, 25, and 30 °C for 24, 48, and 72 h under static conditions. The medium and the planktonic cells were carefully removed with a micropipette, and the wells were washed two times with sterile phosphate-buffered saline (PBS). The tip was inserted slowly to avoid touching the sides and bottom of the wells. The microplates were kept at room temperature overnight and stained for 15 min with 200 μL of crystal violet solution

1% p/v (Biopack, Marbe, Argentina), also at room temperature. The dye solution was removed and each well washed with water. Finally, 200 μL of 100% ethanol were added, and an $\text{OD}_{560\text{nm}}$ reading was done using ELISA equipment (Labsystems Multiskan MS). Each isolate was evaluated in triplicate on the microplate, with a triplicate sample per condition. NCIB3610 was the positive control and JH642 the negative one. Uninoculated wells containing only MSgg or MLB served as blanks.

To analyze the optical density (OD) readings, a cut-off point (ODe) was established as suggested by [70], who consider three standard deviations (SD) of the mean ODc for the following calculation: $\text{ODe} = \text{ODc} + 3 \times \text{SD}$ of the controls. For each culture, the final OD value was expressed as $\text{OD} - \text{ODe}$. Negative values were considered zero, and positive values were interpreted to indicate production of adherent biofilm. *In vitro* biofilm formation was classified thus: no production ($\text{ODs} \leq \text{ODe}$), weak production ($\text{ODe} < \text{ODs} \leq 2\text{ODe}$), moderate production ($2\text{ODe} < \text{ODs} \leq 4\text{ODe}$), and strong production ($4\text{ODe} < \text{ODs}$), following [35] and [70].

2.5. Analysis of bacterial motility

Bacterial motility was assessed according to Ref. [36] in nutrient agar (NA) 0.7% p/v to observe swarming or 0.3% p/v to observe swimming. The inocula were prepared as mentioned previously. For each isolate, two μL of cell suspension at mid-exponential phase were inoculated in the center of Petri plates (9 cm in diameter). The plates were kept upside down at 30 °C for 72 h, and the diameter of the colonies was measured across time. The assays were evaluated in duplicate and repeated four times. NCIB3610 was the control strain for swarming and JH642 for swimming [37]. A strain was considered mobile when the diameter of the colony it formed was at least 20% bigger than that of the colony formed in NB-fortified 1.5% agar [36].

2.6. Statistical analyses

An analysis of variance (ANOVA) was used to evaluate the differences in biofilm formation from one isolate to another and under varying environmental conditions. The mean values of significant differences were compared with a DGC test. For motility, values were expressed as the mean (in centimeters) \pm the SD of four independent experiments in duplicate. Comparisons between isolates were made with one-factor ANOVA and corrected *post-hoc* with a DGC test for multiple comparisons. All the analyses were performed on the software InfoStat (Grupo Infostat, FCA, Universidad Nacional de Córdoba, Argentina). Graphical analyses were made on GraphPad Prism 5.0 (GraphPad Software, San Diego, CA).

3. Results

3.1. Identification of biological control agents (BCAs)

The sequencing of the 16 rRNA gene revealed that EM-A7 (GenBank accession number OL704804) was 99% identical to *B. subtilis* NCIB3610 (CP020102.1). Strains EM-A6 (OL704803) and EM-A8 (OL704805) were 99% identical to *B. velezensis* strain NRRL B-41580 (KY694464.1). The phylogenetic trees can be found in the Supplementary Material (S1). These results agree with the scores >2.000 obtained for the strains through MALDI-TOF MS, which indicate high identification at the species level (Table 1).

3.2. Development of biofilm in the form of pellicles and architecturally complex colonies

Different environmental conditions brought about morphological changes in the pellicles and colonies formed by the strains. These changes were observable in time and space. As seen in Fig. 1, the three isolates (EM-A6, EM-A7, and EM-A8) produced markedly different

Table 1
Molecular and MALDI-TOF identification of *Bacillus* spp.

Isolates	Identification	Length (bp)	Total score	Match/total PMI ^a	Genbank accession number	MALDI-TOF score
EM-A6	<i>B. velezensis</i> (OL704803)	1503	1504	1484/1488 99%	KY694464.1	2.039
EM-A7	<i>B. subtilis</i> (OL704804)	1503	1466	1473/1476 99%	CP020102.1	2.023
EM-A8	<i>B. velezensis</i> (OL704805)	1504	1504	1486/1489 99%	KY694464.1	2.025

^a Percentage of maximum identity of partial 16S rRNA sequence according to Blast database. Base pair (bp).

colonies on biofilm-inducing MSgg agar and MLA. A colony was considered more architecturally complex when it had these characteristics: numerous wrinkles and veins spreading from the center to the edges; a creamy and convex center; lobed and irregular edges; beige in color; and variable size. On the other hand, less complex colonies were also beige but small, smooth, and round, with well-defined edges. Some colonies fell somewhere between these two categories, since they displayed fewer wrinkles and veins than the most complex ones but had a creamy center, irregular to rounded edges, and less intensity of color.

As seen in Fig. 1B, the colonies formed on MSgg agar at 30 °C and $\Psi = -1.38$ MPa were the most architecturally complex. Under those conditions, average colony size was 16 mm for EM-A6, 15 mm for EM-A8, and 11 mm for EM-A7 (Table 2). In general, they were as large as those formed by NCIB3610, which had elevations and opaque wrinkles. In contrast, the colony formed by JH642 was smooth and a lot smaller (5 mm). When temperature and/or water potential were lower, the morphological complexity of all the colonies decreased. Although their diameters varied, they tended to be less wrinkled, with a creamy center, irregular to rounded edges, and no veins from the center to the edges. After 72 h of incubation at 30 °C and water potentials of - 4.19 and - 7.06 MPa, the isolates produced rough but smaller colonies (4–10 mm depending on the strain). The reference strain colonies were small (4–5 mm), smooth, circular and beige, with well-defined edges.

The complexity of the colonies formed by the three isolates on MSgg at 25 °C and $\Psi = -1.38$ MPa was similar to that at 30 °C and the same water potential. However, the maximum diameter was 10 mm (Table 2). The colonies formed by NCIB3610 were even smaller (5–8 mm) and less architecturally complex when temperature decreased to 25 or 20 °C and water potential to $\Psi = - 4.19$ and - 7.06 MPa. Under the same conditions, the colony corresponding to JH642 was smooth and also small (2–4 mm). Essentially, higher temperatures (30 and 25 °C) and the highest water potential value ($\Psi = -1.38$ MPa) led to the formation of more architecturally complex colonies.

The morphology of the colonies formed by all the strains at 30 °C and $\Psi = -1.38$ MPa on MLA was different than on MSgg under the same conditions. They were not smooth, but no wrinkles or veins were observable from the center to the edges. The center, which was more intense in color than the irregular, curvilinear edges, was smooth in some cases and multi-globulated and shiny in others. Some colonies featured a raised, ring-shaped edge. Diameters varied between 5 and 12 mm. For EM-A7 and EM-A8 in particular, they were about 10 and 12 mm. Similarly to what happened on MSgg, lower temperatures (25 and 20 °C) and water potential values ($\Psi = - 4.19$ and - 7.06 MPa) were associated to less architecturally complex colonies on MLA, but many characteristics remained: a more intense, sometimes smooth and multi-globulated center, with ring-shaped or irregular/curvilinear edges. Overall, all the isolates were able to form biofilm on both growth media and under all the conditions tested, but the biofilm's complexity and characteristics were not the same across all strains and conditions.

Fig. 1A shows the development of biofilm in the form of pellicles (or floating biofilm) in MSgg broth, after 72 h of incubation at 30 °C and $\Psi = -1.38$ MPa. For the three isolates as well as NCIB3610, a correlation was observed between formations on the solid-air and liquid-air

interfaces: when the colonies were densely wrinkled, the pellicles were also thicker and more complex. JH642, conversely, was not able to form biofilm. The production of robust pellicles by the isolates was maintained at 25 °C and $\Psi = - 4.19$ MPa. However, when the temperature dropped to 20 °C and the water potential to -7.06 MPa, the pellicles were thin and smooth, lacking a distinctive macroscopic architecture and appearing more fragile or brittle to the naked eye (data not shown).

In MLB, pellicles only developed at 30 °C and $\Psi = -1.38$ and -4.19 MPa. They were thin and not very wrinkly; sometimes brittle and smooth without a distinct macroscopic structure, as was the case at lower temperatures and water potentials in MSgg. These results confirm that the three isolates can produce biofilm in the form of pellicles under different environmental conditions, but their morphology changes from one strain to the other and is influenced by the factors considered.

Biofilm colonies are characterized by their three-dimensional structure and the presence of exopolysaccharides (EPS). We used scanning electron microscopy (SEM) to visualize changes in this structure, in colony architecture and in cell morphology for the three isolates grown on MLA and MSgg agar at 30 °C and $\Psi = -1.38$ MPa (Fig. 2). The architectural complexity shown in the images agrees with the observations made *in vitro*. Bacillary morphology and bacterial distribution were also assessed after 72 h of incubation. In general, biofilms appeared as accumulations of bacteria immersed in an amorphous substance. Bacilli were not isolated from each other but rather grouped in piles as masses of growing cells, with each group connected to others. On MSgg, NCIB3610 cells were longer and thinner than those of EM-A6, EM-A7 and EM-A8, as well as differently distributed. Careful examination of the biofilm surface revealed small groups of spherical granules and rough-looking EPS (see Fig. 2, EM-A7 on MSgg). An abundant accumulation of rough material, which might have contained exopolysaccharides, was visible on the surface of a rough and dense extracellular matrix. As a whole, the results obtained through SEM suggest that the bacterial cells were scattered on a compact biofilm matrix on both growth media.

3.3. Qualitative classification and quantification of biofilm formed under different conditions

The biofilm formed by each strain after 72 h of incubation in MSgg broth and MLB was measured in terms of diameter, quantified and qualitatively classified (Table 2). The isolates were able to produce biofilm in variable forms on both media, at different temperatures and water potentials. Qualitatively, all three were classified as strong/moderate producers at 30 °C, both in MSgg (with percentages between 67 and 100%) and in MLB (33–67%). They also had strong/moderate production at $\Psi = -1.38$ MPa (50% in general), whereas a decrease in water potential well as in temperature (20 °C) rendered them weak. Again, these results indicate that biofilm production by EM-A6, EM-A7 and EM-A8 changes according to temperature, water potential and growth medium. Production by EM-A8 after 72 h of incubation in MSgg at 30 °C and $\Psi = -1.38$ MPa was the highest overall. Its OD_{660nm} values were greater than 2 in MSgg at all Ψ evaluated and 25 and 30 °C. The lowest production values for all the strains were observed at 20 °C in MLB.

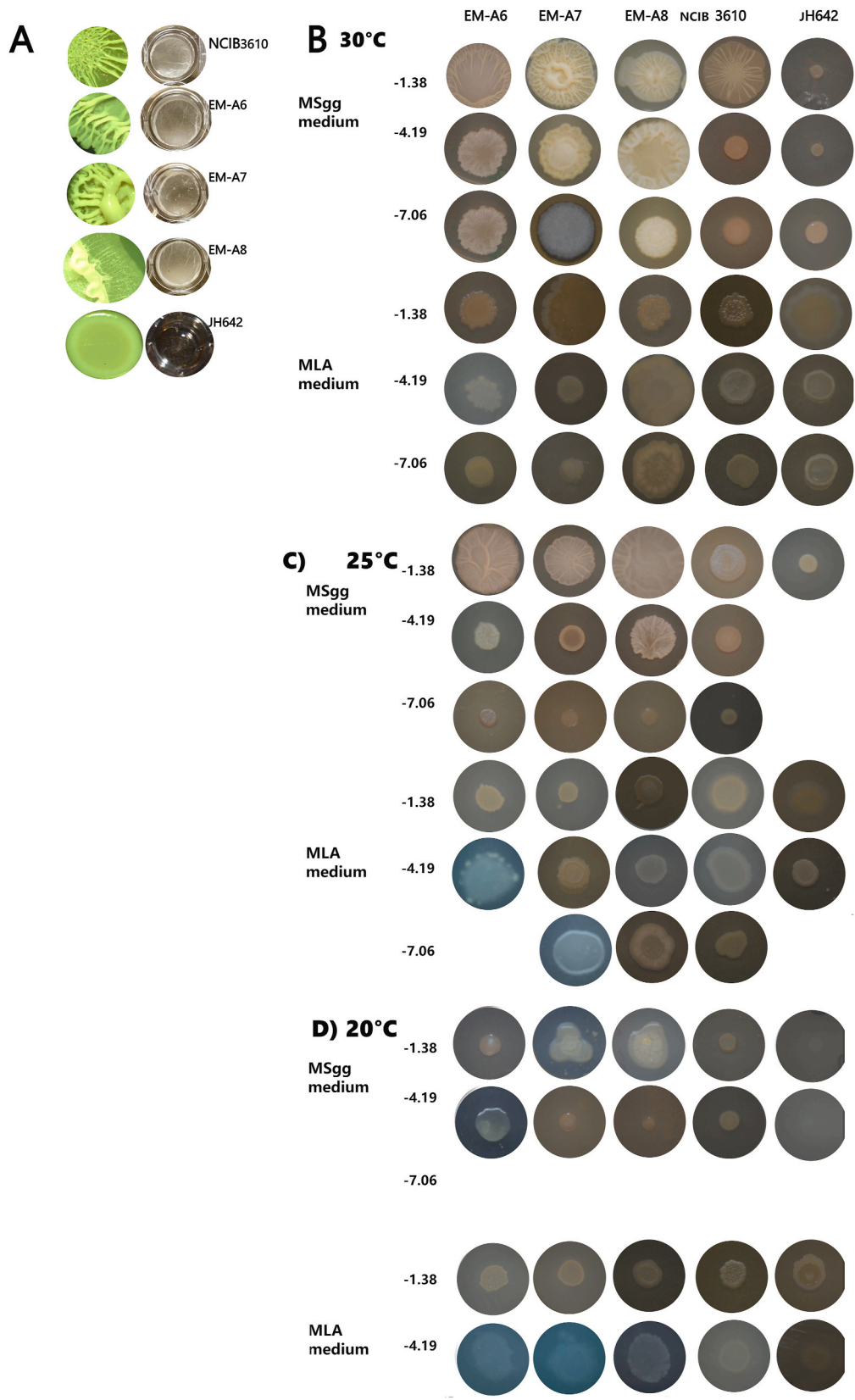


Fig. 1. Biofilm development in the form of pellicles and architecturally complex colonies by *Bacillus subtilis* (EM-A7) and *Bacillus velezensis* (EM-A6 and EM-A8), on different media and at different temperatures and water potentials (Ψ). A) Pellicle development in MSgg broth and MLB after 72 h incubation at 30 °C and $\Psi = -1.38$ MPa. The images obtained with a stereoscopic microscope are representative of triplicate assays performed as three independent experiments. B) Colonies formed on different media at different temperatures and water potentials (Ψ). The images are representative of triplicate assays performed as three independent experiments, and were taken after 72 h of incubation at 30, 25, and 20 °C. The scale bar at the bottom represents 1 cm. MSgg: biofilm-inducing agar; MLA: maize leaves agar; water potential values $\Psi = -1.38, -4.19$ and -7.06 MPa.

Table 2Ability of *B. subtilis* and *B. velezensis* to form biofilm *in vitro* after 72 h of incubation on different culture media, at different temperatures and water potentials.

Strain	Temperature (°C)	Culture medium	Water potential (Ψ)	Colony diameter ± standard deviation (mm)	Values ± standard errors ^a	Biofilm production ability ^b	Proportion of qualitative classification (%) ^c
EM-A6	20 °C	ML	-7.06	3 ± 3	0.025 ± 0.025	NP	0/3
			-4.19	4 ± 3	0.763 ± 0.299	S	0%
			-1.38	5 ± 4	0.140 ± 0.103	NP	
		MSgg	-7.06	0 ± 0	0.225 ± 0.135	NP	1/3
			-4.19	0 ± 0	0.260 ± 0.110	NP	33%
			-1.38	4 ± 0	3.020 ± 0.160	S	
	25 °C	ML	-7.06	4 ± 3	0.250 ± 0.110	NP	0/3
			-4.19	6 ± 4	0.233 ± 0.124	NP	0%
			-1.38	7 ± 2	0.257 ± 0.126	NP	
		MSgg	-7.06	2 ± 1	0.370 ± 0.140	NP	2/3
			-4.19	8 ± 5	1.867 ± 0.643	S	67%
			-1.38	10 ± 3	3.017 ± 0.022	S	
	30 °C	ML	-7.06	4 ± 3	0.445 ± 0.125	W	0/3
			-4.19	9 ± 3	0.680 ± 0.090	W	0%
			-1.38	7 ± 1	0.223 ± 0.105	NP	
		MSgg	-7.06	4 ± 3	1.970 ± 0.160	S	3/3
			-4.19	10 ± 5	2.170 ± 0.760	S	100%
			-1.38	16 ± 0	2.863 ± 0.228	S	
EM-A7	20 °C	ML	-7.06	4 ± 3	0.110 ± 0.060	NP	0/3
			-4.19	5 ± 4	0.120 ± 0.100	NP	0%
			-1.38	7 ± 1	0.397 ± 0.146	NP	
		MSgg	-7.06	0 ± 0	0.285 ± 0.285	NP	1/3
			-4.19	4 ± 1	0.300 ± 0.300	NP	33%
			-1.38	7 ± 1	2.790 ± 0.600	S	
	25 °C	ML	-7.06	4 ± 3	0.700 ± 0.252	W	0/3
			-4.19	4 ± 4	0.463 ± 0.128	W	0%
			-1.38	6 ± 3	0.140 ± 0.087	NP	
		MSgg	-7.06	4 ± 1	1.360 ± 0.820	M	3/3
			-4.19	5 ± 2	1.807 ± 0.688	S	100%
			-1.38	10 ± 0	1.693 ± 0.688	S	
	30 °C	ML	-7.06	6 ± 3	0.265 ± 0.035	NP	1/3
			-4.19	8 ± 4	1.083 ± 0.261	M	33%
			-1.38	8 ± 3	0.027 ± 0.027	NP	
		MSgg	-7.06	4 ± 2	0.300 ± 0.300	NP	2/3
			-4.19	5 ± 0	2.493 ± 0.452	S	67%
			-1.38	11 ± 1	2.747 ± 0.475	S	
EM-A8	20 °C	ML	-7.06	4 ± 4	0.160 ± 0.160	NP	0/0
			-4.19	6 ± 5	0.225 ± 0.225	NP	0%
			-1.38	6 ± 2	0.223 ± 0.088	NP	
		MSgg	-7.06	0 ± 0	0.147 ± 0.079	NP	1/3
			-4.19	2 ± 2	0.150 ± 0.150	NP	33%
			-1.38	6 ± 2	3.047 ± 0.282	S	
	25 °C	ML	-7.06	6 ± 2	0.417 ± 0.217	W	0/3
			-4.19	10 ± 2	0.720 ± 0.290	W	0%
			-1.38	9 ± 4	0.203 ± 0.102	NP	
		MSgg	-7.06	2 ± 2	2.310 ± 0.770	S	3/3
			-4.19	6 ± 6	2.435 ± 0.535	S	100%
			-1.38	18 ± 3	2.936 ± 0.073	S	
	30 °C	ML	-7.06	9 ± 3	1.280 ± 0.050	M	2/3
			-4.19	9 ± 3	0.810 ± 0.350	M	67%
			-1.38	9 ± 2	0.183 ± 0.131	NP	
		MSgg	-7.06	5 ± 2	2.070 ± 1.070	S	3/3
			-4.19	9 ± 6	2.500 ± 0.810	S	100%
			-1.38	16 ± 8	2.813 ± 0.251	S	

An analysis of variance demonstrated that the quantification of the biofilm produced by the isolates was influenced by all five factors: strain, temperature, water potential, growth medium, time, and the interactions between them (Table 3). The most influential factor was the growth medium (GM) ($F = 219.79, P < 0.0001$), followed by water potential ($F = 152.28, P < 0.0001$), time (T) ($F = 122.82, P < 0.0001$) and temperature (T°C) ($F = 106.09, P < 0.0001$). The least influential was strain (S) ($F = 9.80, P = 0.0001$).

^a Values obtained through a crystal violet assay. ODnc at 20 °C ML Ψ - 7.06 = 0.245; ML Ψ - 4.19 = 0.282; Ψ - 1.38 = 0.273; MSgg Ψ - 7.06 = 0.285; Ψ - 4.19 = 0.279; Ψ - 1.38 = 0.245; ODnc at 25 °C ML Ψ - 7.06 = 0.217; Ψ - 4.19 = 0.263; Ψ - 1.38 = 0.237; MSgg Ψ - 7.06 = 0.260; Ψ - 4.19 = 0.277; Ψ - 1.38 = 0.255; ODnc at 30 °C ML Ψ - 7.06 = 0.181; Ψ - 4.19 = 0.217; Ψ - 1.38 = 0.263; MSgg Ψ - 7.06 = 0.230; Ψ - 4.19 = 0.201; Ψ - 1.38 = 0.236.

^b NP: non biofilm producer; W: weak biofilm producer; M: moderate biofilm producer; S: strong biofilm producer.

^c Proportion of mode rate or strong production (%) for each strain at 30 °C, at different water potentials and on different culture media after 72 h of incubation.

Fig. 3 shows the quantification of biofilm expressed as OD_{560nm} values. Biofilm was quantified for all the strains (the three isolates and the two reference strains) incubated in MSgg broth (A) or MLB (B) for different periods. Biofilm production was generally higher in MSgg than in MLB over time. In MSgg (Fig. 3A), production by EM-A6 was the only one that was statistically significant ($P = 0.0009$) between 24 and 48–72 h. A crystal violet assay found no significant differences between

production by EM-A7 and EM-A8. In addition, production by the three isolates was similar to that by NCIB3610. Finally, production values by JH642 were the lowest, and the strain was qualitatively classified as a non-producer.

In MLB (Fig. 3B) at 30 °C and Ψ = -1.38 MPa, the highest quantification was registered at 24 h and corresponded to EM-A6 (1.04). The other two isolates also had their highest values at this time and potential

Table 3

Significance of strain, temperature, water potential, growth medium, time, and the interactions between them on the quantification of biofilm formed by *Bacillus* isolates.

Factor ^a	SC ^b	gl	CM	F	P
S	4.31	2	2.16	9.80	0.0001
T°C	46.73	2	23.36	106.09	<0.0001
Ψ	67.07	2	33.54	152.28	<0.0001
GM	48.40	1	48.40	219.79	<0.0001
T	54.10	2	27.05	122.82	<0.0001
S*T°C	0.95	4	0.24	1.08	0.3680
S*Ψ	2.12	4	0.53	2.40	0.0504
S*GM	0.56	2	0.28	1.28	0.2795
S*T	9.25	4	2.31	10.50	<0.0001
T°C*Ψ	15.94	4	3.98	18.10	<0.0001
T°C*GM	1.49	2	0.74	3.37	0.0359
T°C*T	2.26	4	0.57	2.57	0.0386
Ψ*GM	67.56	2	33.78	153.40	<0.0001
Ψ*T	6.98	4	1.74	7.92	<0.0001
GM*T	23.74	2	11.87	53.89	<0.0001
S*T°C*Ψ	6.16	8	0.77	3.50	0.0008
S*T°C*GM	0.15	4	0.04	0.17	0.9528
S*T°C*T	11.91	8	1.49	6.76	<0.0001
S*Ψ*GM	4.31	4	1.08	4.89	0.0008
S*Ψ*T	4.30	8	0.54	2.44	0.0148
S*GM*T	2.80	4	0.70	3.18	0.0142
T°C*Ψ*GM	3.44	4	0.86	3.90	0.0043
T°C*GM*T	4.46	4	1.11	5.06	0.0006
S*T°C*Ψ*GM	6.77	8	0.85	3.84	0.0003
S*T°C*Ψ*T	12.43	16	0.78	3.53	<0.0001
S*T°C*GM*T	5.09	8	0.64	2.89	0.0043
S*Ψ*GM*T	6.44	8	0.80	3.65	0.0005
T°C*Ψ*GM*T	11.68	8	1.46	6.63	<0.0001
S*T°C*Ψ*GM*T	11.06	16	0.69	3.14	0.0001

^a S: strain; T°C: temperature; Ψ: water potential; GM: culture medium; T: time.

^b SC: means of the squares.

(1.16 for EM-A7, 0.91 for EM-A8). The differences in these values were not statistically significant, and production by all three decreased after 48 and 72 h. In the case of JH642, OD_{560nm} values were similar at 24 and 48 h (weak production) and were reduced further after 72 h (no production). Meanwhile, there were no statistically significant differences over time ($P < 0.05$) for NCIB3160. A crystal violet assay of all the cultures in MLB rendered lower production values over time than in MSgg.

Fig. 4A compares biofilm quantification between the strains, after they were incubated for 72 h in MSgg broth at $\Psi = -1.38$ and different temperatures (20, 25, and 30 °C). At 30 °C, the values for the three isolates were similar to that for NCIB3610 and significantly higher than for JH642 ($P < 0.0001$). Quantification for the two *B. velezensis* strains (EM-A6 and EM-A8) was similar, with values between 2.408 and 3.342 and no statistically significant differences at varying temperatures ($P > 0.05$). On the other hand, differences were significant between those two strains and *B. subtilis* EM-A7 at 25 °C ($P < 0.0001$). In fact, EM-A7 had the lowest quantification at this time. Once again, JH642 was a weak producer at 25 and 20 °C. At the same temperatures, NCIB3610 continued being able to produce biofilm but at lower values than our strains, with significant differences between 20 and 25 °C ($P = 0.0016$ and $P < 0.05$). As mentioned earlier, quantification values were generally lower in MLB than in MSgg broth for all the strains at the three temperatures evaluated.

Fig. 5 shows how biofilm formation was affected by modifying water potential in the growth media, after 72 h of incubation at 30 °C. The effects of this change did not vary significantly from one isolate to the other in MSgg ($P > 0.05$). Quantification for EM-A7 was significantly lower when potential decreased from $\Psi = -1.38$ MPa to - 4.19 and - 7.06 MPa. There were no statistically significant differences between production by the three isolates and by NCIB3610 at $\Psi = -1.38$ MPa and $\Psi = - 4.19$ MPa. Out of all the strains, quantification was the lowest for JH642 across all water potential values. At $\Psi = - 4.19$ MPa and - 7.06

MPa, statistically significant differences emerged between our strains and the reference ones. Once again, biofilm production in MLB was overall lower than in MSgg. In this medium, the highest production by EM-A7 was registered at $\Psi = - 4.19$ MPa, while for EM-A8 it was at $\Psi = - 7.06$ MPa, both at 30 °C.

3.4. Analysis of bacterial motility

The strains' motility was evaluated on two media with different agar concentrations (0.3% for swimming, 0.7% for swarming), using NCIB3610 as the control for swarming and JH642 as a control for swimming. EM-A6, EM-A7 and EM-A8 were able to both swim and swarm (Fig. 6), with statistically significant differences between them ($P < 0.0001$). On 0.7% agar, the diameters of the colonies formed by EM-A7, EM-A8, and NCIB3610 were significantly different than for EM-A6 (Fig. 6A). Colonies by all three of our strains, nevertheless, were 20% bigger than those they formed on 1.5% agar (Fig. 6B), which was the established criterion to identify swarming. By contrast, JH642 was not able to swarm, and its colonies were about 1 cm in diameter on the two media (Fig. 6A and B). Fig. 6C shows changes in colony diameter for each strain over time. The highest values overall were registered at 30 °C and belonged to EM-A7 and EM-A8; 9 cm after 20 h on 0.3% agar; 8 and 7 cm after 40 h on 0.7% agar. In the case of EM-A6, its biggest diameter was recorded after 20 h on the swimming medium and after 72 h on the swarming medium.

4. Discussion

Biocontrol strategies, which are based on the use of BCAs against plant pathogens, would benefit from further research on the interaction between the biological agent, the pathogen and the plant. In the case of maize, a better understanding of how potentially beneficial bacteria behave and function in its phyllosphere could help predict the degree of protection they would offer the plant against pathogenic infection.

Selecting a potential biocontrol microorganism involves a series of steps such as isolation, conservation, identification, preliminary risk analysis, and ecophysiological characterization [38]. In this study, a proteomic- and a genetic-based approach were used to complete the identification of three *Bacillus* spp. isolates from the maize phyllosphere (EM-A6, EM-A7, and EM-A8). In the last 30 years, classifications within this genus have been substantially revised because it contains several groups of closely related species, which share a pattern of morphological, biochemical and genetic characteristics [39]. For instance, the members of *B. subtilis* (which include *B. subtilis* subsp. *subtilis*, *B. amyloliquefaciens*, and *B. licheniformis*) cannot be distinguished on the basis of their 16S rRNA gene sequences alone, since they are more than 99% similar [40,69]. We identified EM-A7 as *B. subtilis* on the basis of both this sequencing and concordant MALDI-TOF scores. However, while 16S rRNA sequencing indicated that EM-A6 and EM-A8 were highly similar to *B. velezensis*, MALDI-TOF pointed towards *B. amyloliquefaciens*. Although protein profiling on MALDI-TOF has proven reliable to identify closely related species including *Bacillus* spp., commercial databases and programs are mainly designed to identify clinical strains [40,41], which would explain the lack of agreement in our results. Moreover, there might be an "operational group *B. amyloliquefaciens*" that includes *B. amyloliquefaciens*, *B. siamensis*, and *B. velezensis*, the main agent in agricultural bioformulations to protect plant health and stimulate plant growth [39,42].

We then assessed the ability of the three isolates to form biofilm. Biofilm is known to enhance bacterial tolerance to changing environmental conditions and thus survival. Biofilm-forming biological agents, therefore, might be more persistent on the leaf surface and have a better chance at protecting the plant against pathogens. This is why the design of foliar applications for biocontrol would be well-served by an increased understanding of this lifestyle in potential BCAs.

The environmental conditions tested here were selected by

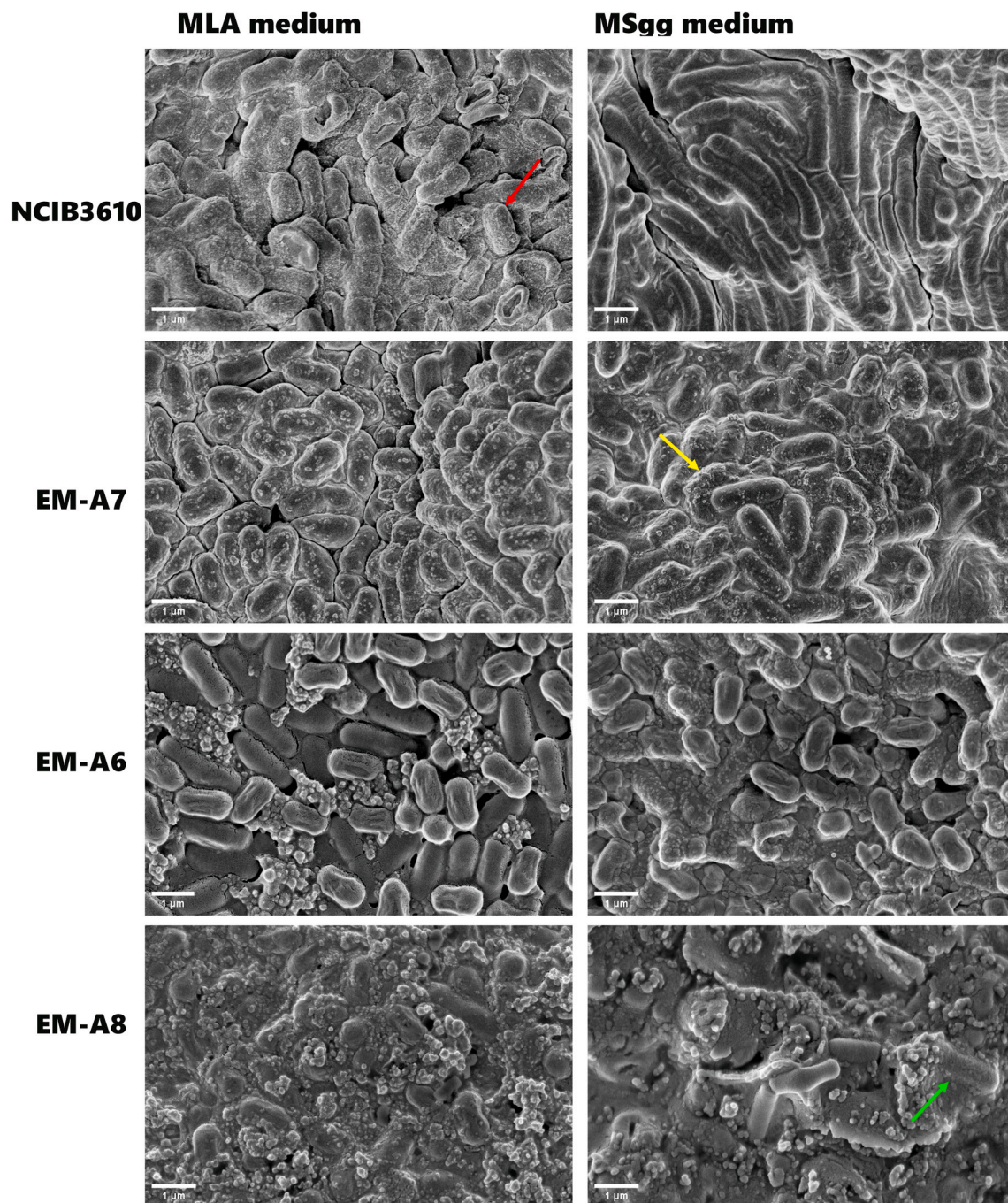


Fig. 2. Scanning electron micrographs of colonies formed by *Bacillus subtilis* (NCIB3610 and EM-A7) and *Bacillus velezensis* (EM-6 and EM-A8) on biofilm-inducing MSgg agar and maize leaves agar (MLA) after 72 h of incubation at 30 °C and $\Psi = -1.38$ MPa. Red arrow: bacillary cell; yellow arrow: EPS granules; green arrow: extracellular polymeric substance.

considering the niche from which the strains were isolated. The assays showed that the isolates are able to grow well at water potentials and temperatures that favor the proliferation of *E. turcicum* on maize fields [43]. Water potential is likely one of the most highly fluctuating factors on leaf surfaces. The EPS slime in biofilm aggregates may buffer bacteria from the dissection stress produced by these changes [44]. As regards temperature, we observed earlier that different isolates of *E. turcicum* could grow between 15 and 30 °C, with the maximum growth rate occurring at 25 °C [45]. Bacteria able to overcome the stress created by this temperature range would afford a significant ecological advantage against the pathogen. On top of withstanding changing water and temperature conditions, EM-A6, EM-A7 and EM-A8 were also able to

produce biofilm on different growth media over time. Their ability to adapt to both environmental and nutritional modifications, then, is likely to enhance their beneficial action in the phyllosphere.

Biofilm formation by *Bacillus* spp. has been studied from different approaches. Some researchers have focused on colonies that grow on agar surfaces and their macroscopically complex architecture, associated with the production of an extracellular matrix [46]. Others have explored the formation of floating, structured pellicles on the liquid-air interface [29,46–48]. Here, we combined approaches to improve the robustness of our results. In general, different conditions in terms of temperature, water potential, growth media and time led to variations in the development of biofilm by the isolates, both on the solid-air and

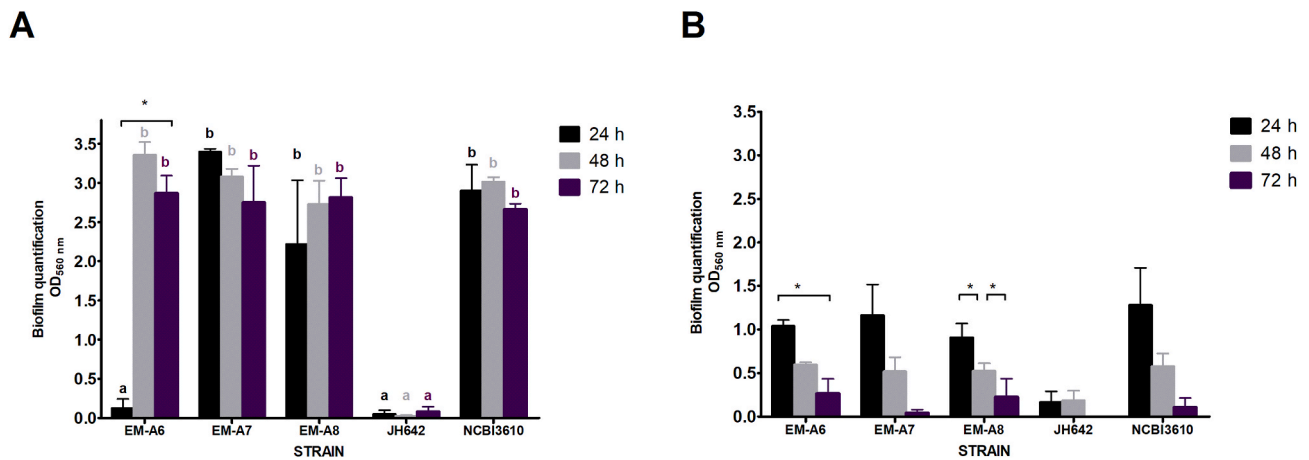


Fig. 3. Quantification of *in vitro* biofilm formation by *Bacillus subtilis* and *Bacillus velezensis* in MSgg broth (A) and MLB (B), after different periods of incubation at 30 °C and $\Psi = -1.38$ MPa. Each bar represents the arithmetic mean \pm standard error (SEM) of the mean of three independent experiments performed in triplicate, expressed as OD_{560nm} values. NCIB3610 was the positive control and JH642 the negative one. The nominal *P*-value for statistical significance was *P* < 0.05, indicated with different letters for strains compared at the same incubation time. Each time is marked with a different color. Square brackets and * indicate statistically significant differences (*P* < 0.05) between changes in each factor for each strain. MSgg: biofilm-inducing broth; MLB: maize leaves broth.

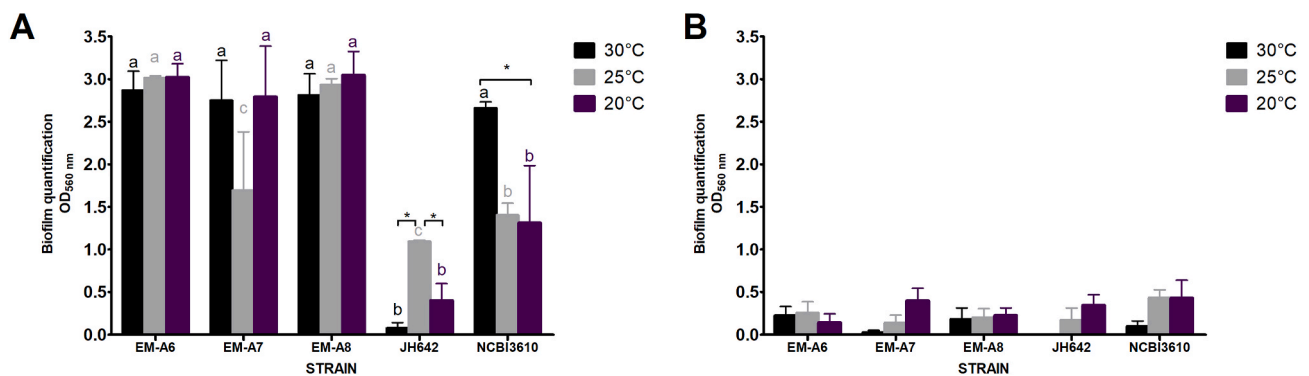


Fig. 4. Quantification of *in vitro* biofilm formation by *Bacillus subtilis* and *Bacillus velezensis* in MSgg (A) and MLB (B), after 72 h of incubation at $\Psi = -1.38$ MPa and different temperatures. Each bar represents the arithmetic mean \pm standard error (SEM) of the mean of three independent experiments performed in triplicate, expressed as OD_{560nm} values. NCIB3610 was the positive control and JH642 the negative one. The nominal *P*-value for statistical significance was *P* < 0.05, indicated with different letters for strains compared at the same temperature. Each temperature is marked with a different color. Square brackets and * indicate statistically significant differences (*P* < 0.05) between changes in each factor for each strain. MSgg: biofilm-inducing broth; MLB: maize leaves broth.

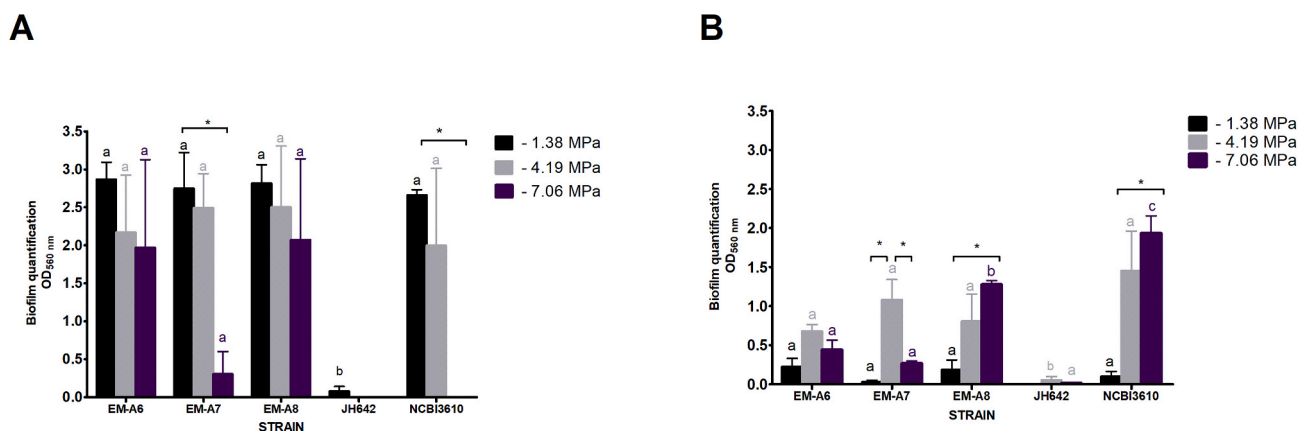


Fig. 5. Quantification of *in vitro* biofilm formation by *Bacillus subtilis* and *Bacillus velezensis* in MSgg broth (A) and MLB (B), after 72 h of incubation at 30 °C and different water potentials (Ψ). Each bar represents the arithmetic mean \pm standard error (SEM) of the mean of three independent experiments performed in triplicate, expressed as OD_{560nm} values. NCIB3610 was the positive control and JH642 the negative one. The nominal *P*-value for statistical significance was *P* < 0.05, indicated with different letters for strains compared at the same water potential. Each water potential value is marked with a different color. Square brackets and * indicate statistically significant differences (*P* < 0.05) between changes in each factor for each strain. MSgg: biofilm-inducing broth; MLB: maize leaves broth.

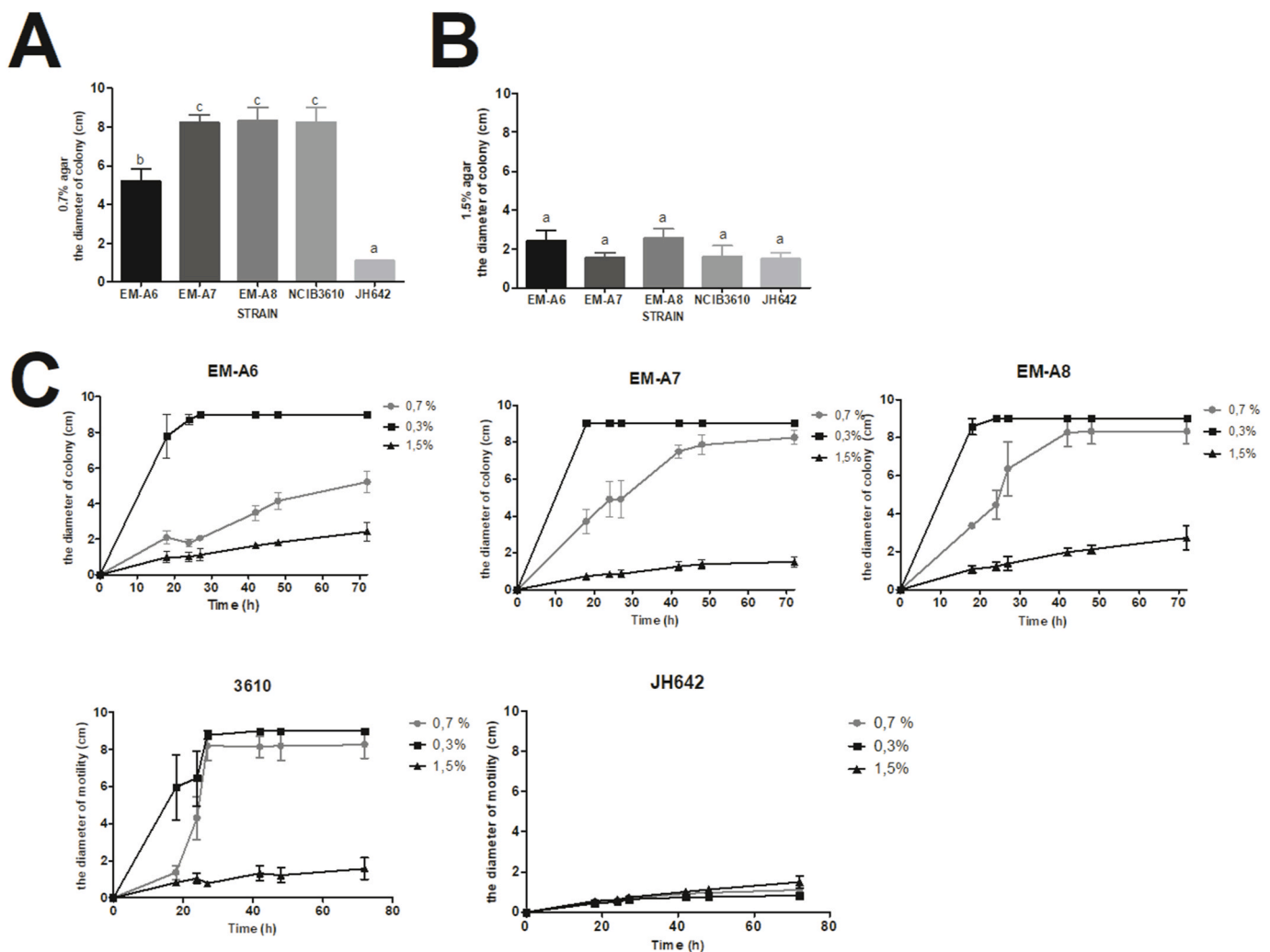


Fig. 6. Motility assays. A) Swarming. Means of the diameter of colonies formed by *Bacillus subtilis* (EM-A7, NCIB3610, and JH642) and *Bacillus velezensis* (EM-A6, EM-A8) on 0.7% nutritive agar (NA), after 72 h of incubation at 30 °C. B) Diameter of disc by *B. subtilis* (EM-A7, NCIB3610, JH642) and *B. velezensis* (EM-A6, EM-A7) on 1.5% nutrient agar (NA), after 72 h of incubation at 30 °C. C) Motility of EM-A6, EM-A7, EM-A8, NCIB3610 and JH642. Mean of disc diameter \pm SEM from four experiments performed in duplicate for 72 h at 30 °C. The nominal *P*-value for statistical significance was $P < 0.05$, indicated with different letters.

liquid-air interfaces.

Scanning electron microscopy (SEM) was used to observe the morphology of colonies and pellicles formed by the three isolates. Conventional SEM is widely used to visualize biofilm morphology in highly magnified detail ($>10,000\times$). However, given that its protocols include dehydration and sputter coating using metal, care must be taken when preparing samples with a high water content (such as biofilm, which is 97% water) to prevent sample loss, collapse, or alteration of real morphology. Dehydration could make EPSs appear as a network of fibers instead of a firm gelatinous matrix [28,49,50].

The images taken at 30 °C and $\Psi = -1.38$ MPa show that the three isolates produced abundant accumulations of rough material, which may have contained exopolysaccharides, on the surface of a rough and dense extracellular matrix. The bacterial cells appeared scattered in a biofilm matrix on the compact surface of the MLA and MSgg agar. This is consistent with other studies that described the cells in wild-type pellicles as “completely enveloped in thick sheets of extracellular material” [28,32].

On MSgg, a synthetic biofilm-inducing medium, the isolates' colonies were as large as those developed by NCIB3610. They were opaque and wrinkled, with tongue-like columns protruding from the agar surface. *B. subtilis* and its related species exhibit a variety of morphological phenotypes, ranging from thin, flat microstructures to large, spatially

heterogeneous colonies. Although not enough is known about the functional structures of these different morphologies [15,31,51], we do know that wrinkles, associated with localized cell death, are one of the most recognizable characteristics of the more complex formations [52]. Wrinkles may enhance structural integrity and elasticity, liquid transport, hydrophobicity, and protection from infiltration by other species [51]. The channels below wrinkles might facilitate the flow of liquid toward the center of the biofilm, and thus nutrient and oxygen transport [53,54]. Opaque wrinkles in particular, like the ones we observed, have been associated with increased sporulation as the biofilm matures [55]. The fact that the three isolates studied here were able to form biofilm with this level of complexity and these features under specific conditions is promising for their use as BCAs in the phyllosphere.

We also detected a correlation between the complexity of colonies and that of pellicles. When the colonies were densely wrinkled, the pellicles were also denser and more complex. Similarly [29], observed at a high magnification that pellicles formed by *Bacillus* spp. in MSgg were mainly composed of long cell chains aligned in parallel. The same authors described a clear correlation between highly structured morphologies and the ability of a cell to produce an extracellular matrix [32]. When water potential and temperature were lower, the appearance of the biofilms changed, i.e. the specific phenotypes of *B. subtilis* colony-type biofilms are determined by environmental factors.

Nutrient availability is also known to influence biofilm phenotype. [56] reported changes in thickness, rim organization and distribution of cell phenotypes within a mature macrocolony at different nutrient levels. [51] described changing rates of spatial expansion depending on the existing nutrients. By modelling biofilm surface morphology with confocal and multiphoton microscopy, they found that nutrient-depleted media triggered the formation of large, straight wrinkles connecting the core and the periphery of the colony [51]. The use of synthetic MSgg allowed us to observe biofilm formation in an ideal medium in terms of nutrients. However, since studies on artificial substrates may not accurately reflect growth ability on natural substrates [57], we contrasted our results with those obtained on MLA, which was meant to replicate the nutrients naturally found on maize leaves.

On MLA at 30 °C and $\Psi = -1.38$ MPa the strains were able to produce biofilm, but this time the colonies had no wrinkles or veins from the center to the edge, which might mean that the nutrient content in leaves is not altogether suitable for the emergence of this kind of phenotype. Still, the ML medium can only approximate the actual nutrients found in the phyllosphere, which may be somewhat affected by laboratory conditions. Moreover, although colony morphology was evidently different on one medium and the other, the strains did not produce flat colonies on MLA. In other words, they were still capable of forming biofilm when subjected to natural-like nutrient availability, in contrast to the negative control (JH642). Thus, colony complexity might be differentially expressed according to nutrient content. One way or another, this kind of information about the nutritional requirements for biofilm formation (as well as water potential and temperature requirements), may be useful to optimize future bacterial formulations. Optimization involves applying strategies to enhance or maintain biocontrol efficiency, including increasing tolerance to environmental stress [71].

The biofilm produced under varying conditions across time was then quantified spectrophotometrically, using microtiter plates and 1% p/v crystal violet staining [35,58]. Spectrophotometry makes it possible to quantify total biofilm mass by observing how dye binds to cells and to negatively charged molecules, such as polysaccharides in the biofilm matrix [34,35]. Crystal violet values were higher for biofilm formed in MSgg than MLB over time. This was expected given the biofilm-inducing nature of MSgg. In both media, nevertheless, the values for the isolates were higher than those of the negative control or the uninoculated media, which suggests that the quantification is indicative of biofilms adhered to the surface.

Finally, the isolates proved capable of swimming and swarming in 0.3 and 0.7% nutrient agar, respectively. Previous studies also observed these abilities in *B. subtilis* and *B. velezensis* [36,37,59]. Motility allows microorganisms to reach more favorable sites on leaf surfaces, and is likely assisted by chemotaxis towards nutrients or plant signaling molecules. Swarming in particular consists of specific collective, coordinated patterns of rapid movement or migration on a surface (2–10 mm h⁻¹), and is a remarkable example of cooperative behavior [48,60]. Nevertheless, the extent to which motility benefits epiphytic fitness in commensal bacteria is not clear. While swarming, adherence and biofilm production all contribute to efficient colonization [61,62], some authors have suggested that flagellar and swarming motility may be relevant but not essential for biofilm formation by *B. subtilis* [63]. On the other hand [64], posited that these processes are coordinated in space and time: first, genes that facilitate motility are expressed; then, matrix production is activated; finally, spores appear on the upper aerial structures of the biofilm.

All in all, the results described here further our knowledge about biofilm production by *Bacillus* isolates with antagonistic potential against common maize leaf pathogens like *E. turcicum*. Other studies have come up with similar findings for other BCA strains. *B. subtilis* 6051 formed extense and stable biofilm that could protect plants from attacks by *Pseudomonas syringae* [65], and NCIB3610 produced robust biofilm on the surface of tomato roots [66]. *B. velezensis* QST713 developed

biofilm on inert surfaces and helped to inhibit the growth of *Trichoderma aggressivum*, which causes green mold disease [67]. [72] similarly suggested that *B. velezensis* could reduce the severity of plant disease by forming biofilm. The use of such microbial antagonists as biological control agents is a promising alternative to pesticides, which often become accumulated in plants and end up affecting humans directly or indirectly [48,68].

5. Conclusion

Three strains isolated from the maize phyllosphere, identified as *B. subtilis* and *B. velezensis* and previously selected as potential biocontrol agents against *E. turcicum*, proved capable of motility and biofilm formation under changing conditions regarding temperature, water potential, and nutrient availability. Evidence on the ability of BCAs to form biofilm, and thus adapt and survive in the face of adverse abiotic factors, is important for the design of consistent and effective biocontrol strategies against plant pathogens. Other studies are currently underway in our laboratory, aimed at investigating the effects of light quality on biofilm formation on maize leaves. This and other research lines should allow us to have a more accurate picture of the ecology of microorganisms in the phyllosphere, and of their potential uses in agricultural practices.

CRedit authorship contribution statement

Aluminé Fessia: designed the project, developed the experiments, and wrote the manuscript. **Melina Sartori:** designed the project and wrote the manuscript. **Daiana García:** designed the project and wrote the manuscript. **Luciana Fernández:** designed the scanning electron microscopy experiments. **Rodrigo Ponzio:** designed the scanning electron microscopy experiments. **Germán Barros:** designed the project and wrote the manuscript, and. **Andrea Nesci:** designed the project and wrote the manuscript.

Declaration of competing interest

No conflict of interest to declare.

Data availability

Data will be made available on request.

Acknowledgments

This work was supported by grants from SECyT-UNRC PPI 2020–2022 (Res. 357/20) and Agencia Nacional de Promoción Científica y Tecnológica (PICT 2018–04220).

Appendix A. Supplementary data

Supplementary data to this article can be found online at <https://doi.org/10.1016/j.biofilm.2022.100097>.

References

- [1] Kovács ÁT, Dragoš A. Evolved Biofilm: review on the experimental evolution studies of *Bacillus subtilis* pellicles. *J Mol Biol* 2019;431(23):4749–59.
- [2] Adnan M, Morton G, Singh J, Hadi S. Contribution of rpoS and bolA genes in biofilm formation in *Escherichia coli* K-12 MG1655. *Mol Cell Biochem* 2010;342:207–13.
- [3] Morris CE, Monier JM, Jacques MA. A technique to quantify the population size and composition of the biofilm component in communities of bacteria in the phyllosphere. *Appl Environ Microbiol* 1998;64:4789–95.
- [4] Fett WF. Naturally occurring biofilms on alfalfa and other types of sprouts. *J Food Protect* 2000;63:625–32.
- [5] Monier JM, Lindow SE. Aggregates of resident bacteria facilitate survival of immigrant bacteria on leaf surfaces. *Microb Ecol* 2005;49:343–52.

- [6] Chaudhry V, Runge P, Sengupta P, Doehlemann G, Parker JE, Kemen E. Shaping the leaf microbiota: plant-microbe-microbe interactions. *J Exp Bot* 2021;72:36–56.
- [7] Bartolini M, Cogliati S, Vileta D, Bauman C, Ramirez W, Grau R. Stress responsive alternative sigma factor SigB plays a positive role in the antifungal proficiency of *Bacillus subtilis*. *Appl Environ Microbiol* 2019;85(9). e00178-19.
- [8] Morris CE, Monier JM. The ecological significance of biofilm formation by plant-associated bacteria. *Annu Rev Phytopathol* 2003;41:429.
- [9] Thapa S, Prasanna R. Prospecting the characteristics and significance of the phyllosphere microbiome. *Ann Microbiol* 2018;68(5):229–45.
- [10] Andrews JH, Harris RF. The ecology and biogeography of microorganisms on plant surfaces. *Annu Rev Phytopathol* 2000;38:145.
- [11] Hirano SS, Upper CD. Bacteria in the leaf ecosystem with emphasis on *Pseudomonas syringae* —a pathogen, ice nucleus, and epiphyte. *Microbiol Mol Biol Rev* 2000;64:624–53.
- [12] Hashem A, Tabassum B, Fathi Abd Allah E. *Bacillus subtilis*: a plant-growth promoting rhizobacterium that also impacts biotic stress. *Saudi J Biol Sci* 2019;26(6):1291–7.
- [13] Pfeilmeier S, Caly DL, Malone JG. Bacterial pathogenesis of plants: future challenges from a microbial perspective: challenges in bacterial molecular plant pathology. *Mol Plant Pathol* 2016;17:1298–313.
- [14] Trabelsi D, Mhamdi R. Microbial inoculants and their impact on soil microbial communities: a review. *BioMed Res Int* 2013;2013:863240.
- [15] Bridier A, Le Coq D, Dubois-Brissonnet F, Thomas V, Aymerich S, Briandet R. The spatial architecture of *Bacillus subtilis* biofilms deciphered using a surface-associated, model and *in situ* imaging. *PLoS One* 2011;6:e16177.
- [16] Habimana O, Guillier L, Kulakauskas S, Briandet R. Spatial competition with *Lactococcus lactis* in mixed-species continuous-flow biofilms inhibits *Listeria monocytogenes* growth. *Biofouling* 2011;27:1065–72.
- [17] Velmourougane K, Prasanna R, Saxena AK. Agriculturally important microbial biofilms: present status and future prospects. *J Basic Microbiol* 2017;57(7):548–73.
- [18] Pertot I, Puopolo G, Hosni T, Pedrotti L, Jourdan E, Ongena M. Limited impact of abiotic stress on surfactin production in planta and on disease resistance induced by *Bacillus amyloliquefaciens* S499 in tomato and bean. *FEMS Microbiol Ecol* 2013;86:505–19.
- [19] Bolsa de Comercio de Rosario (BCR). Available in, <https://www.bcr.com.ar/es/mecadocs/investigacion-y-desarrollo/informativo-semanal/noticias-informativo-semanal/argentina-se; 2021>.
- [20] Navarro BL, Ramos Romero L, Kistner MB, Iglesias J, von Tiedemann A. Assessment of physiological races of *Exserohilum turcicum* isolates from maize in Argentina and Brazil. *Trop Plant Pathol* 2021;46:371–80.
- [21] Sartori M, Nesci A, Formento A, Etcheverry M. Selection of potential biological control of *Exserohilum turcicum* with epiphytic microorganisms from maize. *Rev Argent Microbiol* 2015;47:62–71.
- [22] Sartori M, Nesci A, Garcia J, Passone MA, Montemaraní A, Etcheverry M. Efficacy of epiphytic bacteria to prevent northern leaf blight caused by *Exserohilum turcicum* in maize. *Rev Argent Microbiol* 2017;49:75–82.
- [23] Sartori M, Nesci Andrea N, Montemaraní A, Barros G, García J, Etcheverry M. Preliminary evaluation of biocontrol agents against maize pathogens *Exserohilum turcicum* and *Puccinia sorghii* in field assays. *08 Agric Sci* 2017:1003–13.
- [24] Sartori M, Bonacci M, Barra P, Fessia A, Etcheverry M, Nesci A, Barros G. Studies on possible modes of action and tolerance to environmental stress conditions of different biocontrol agents of foliar diseases in maize. *Agric Sci* 2020;11:552–66.
- [25] Holt JG, Krieg NR, Sneath PHA, Staley J, Williams ST. In: Bergey's manual of determinative Bacteriology, group 17: gram-positive cocci and group 18: endospore-forming gram-positives and cocci. 9th edition. Baltimore, Md, USA: Williams and Wilkins; 1994. 527–64.32J.
- [26] Rocca MF, Almuzara M, Barberis C, Vay C, Viñes P, Prieto M. Presentación del sitio web de la Red Nacional de Identificación Microbiológica por Espectrometría de Masas. Manual para la interpretación de resultados de MALDI-TOF MS. *Rev Argent Microbiol* 2020;52:83–4.
- [27] Beauregard PB, Chai Y, Vlamakis H, Losick R, Kolter R. *Bacillus subtilis* biofilm induction by plant polysaccharides. *Proc Natl Acad Sci U S A* 2013;110:1621–30.
- [28] Bucher T, Kartvelishvily E, Kolodkin-Gal I. Methodologies for studying *B. Subtilis* biofilms as a model for characterizing small molecule biofilm inhibitors. *JoVE* 2016;1–11.
- [29] Branda SS, González-Pastor JE, Ben-Yehuda S, Losick R, Kolter R. Fruiting body formation by *Bacillus subtilis*. *Proc Natl Acad Sci U S A* 2001;98:11621–6.
- [30] Lemon KP, Earl AM, Vlamakis HC, Aguilar C, Kolter R. Biofilm development with an emphasis on *Bacillus subtilis*. In: Current topics in microbiology and immunology; 2008. p. 1–16.
- [31] Gallegos-Monterrosa R, Mhatre E, Kovács ÁT. Specific *Bacillus subtilis* 168 variants form biofilms on nutrient-rich medium. *Microbiology* 2016;162:1922–32.
- [32] Branda SS, Chu F, Kearns DB, Losick R, Kolter R. A major protein component of the *Bacillus subtilis* biofilm matrix. *Mol Microbiol* 2006;59:1229–38.
- [33] Zhu ML, Wu XQ, Wang YH, Dai Y. Role of biofilm formation by *Bacillus pumilus* HR10 in biocontrol against pine seedling damping-off-disease caused by *Rhizoctonia solani*. *Forests* 2020;11:1–17.
- [34] Allkja J, Bjarsholt T, Coenye T, Cos P, Fallarero A, Harrison JJ, Lopes SP, Oliver A, Pereira MO, Ramage G, Shirtliff ME, Stoodley P, Webb JS, Zaat SAJ, Goeres DM, Azevedo NF. Minimum information guideline for spectrophotometric and fluorometric methods to assess biofilm formation in microplates. *Biofilms* 2020;2:100010.
- [35] Stepanović S, Vuković D, Dakić I, Savić B, Švabić-Vlahović M. A modified microtiter-plate test for quantification of staphylococcal biofilm formation. *J Microbiol Methods* 2000;40:175–9.
- [36] Bartolini M, Grau R. Assessing different ways of *Bacillus subtilis* spreading over abiotic surfaces. *Bio-Protocol* 2019;9:1–10.
- [37] Grau RR, De Oña P, Kunert M, Leñini C, Gallegos-Monterrosa R, Mhatre E, Vileta D, Donato V, Hölischer T, Boland W, Kuipers OP, Kovács ÁT. A duo of potassium-responsive histidine kinases govern the multicellular destiny of *Bacillus subtilis*. *mBio* 2015;6:1–16.
- [38] Cotes AM, Fargetton X, Köhl J. Diseño conceptual, selección y prueba de concepto de microorganismos biocontroladores. In: Cotes AM, editor. Control biológico de fitopatógenos, insectos y ácaros. Volumen 2 Agentes de control biológico. Bogotá, Colombia: Agrosavia; 2018. p. 598–624.
- [39] Fan B, Blom J, Klenk HP, Borriss R. *Bacillus amyloliquefaciens*, *Bacillus velezensis*, and *Bacillus siamensis* form an 'operational group *B. amyloliquefaciens*' within the *B. subtilis* species complex. *Front Microbiol* 2017;8:1–15.
- [40] Starostin KV, Demidov EA, Bryanskaya AV, Efimov VM, Rozanov AS, Peltek SE. Identification of *Bacillus* strains by MALDI TOF MS using geometric approach. *Sci Rep* 2015;5:1–9.
- [41] Celandroni F, Vecchione A, Cara A, Mazzantini D, Lupetti A, Ghelardi E. Identification of *Bacillus* species: implication on the quality of probiotic formulations. *PLoS One* 2019;14(5):e0217021.
- [42] Fan B, Wang C, Song X, Ding X, Wu L, Wu H, Gao X, Borriss R. *Bacillus velezensis* FZB42 in 2018: the gram-positive model strain for plant growth promotion and biocontrol. *Front Microbiol* 2018;9:2491.
- [43] Couretot L, Parisi L, Hirsch M, Suarez ML, Magnone G, Ferraris G. Principales enfermedades del cultivo de maíz en las últimas campañas y su manejo. 2013. p. 7. <http://inta.gov.ar/documentos/principalesenfermedades-del-cultivo-de-maiz-en-las-ultimas-campanas-y-su-manejo> Acces Octubre 2022.
- [44] Lindow SE, Brandt MT. Microbiology of the phyllosphere. *Appl Environ Microbiol* 2003;69(4):1875–83.
- [45] Montemaraní A, Sartori M, Nesci A, Etcheverry M, Barros G. Influence of crop residues, matric potential and temperature on growth of *Exserohilum turcicum* an emerging maize pathogen in Argentina. *Lett Appl Microbiol* 2018;67(6):614–9.
- [46] Kearns DB, Chu F, Branda SS, Kolter R, Losick R. A master regulator for biofilm formation by *Bacillus subtilis*. *Mol Microbiol* 2005;55:739–49.
- [47] Thérien M, Kiesewalter HT, Auria E, Charon-Lamoureux V, Wibowo M, Maróti G, Kovács ÁT, Beauregard PB. Surfactin production is not essential for pellicle and root-associated biofilm development of *Bacillus subtilis*. *Biofilms* 2020;2:100021.
- [48] Dergham Y, Sanchez-Vizuete P, Le Coq D, Deschamps J, Bridier A, Hamze K, Briandet R. Comparison of the genetic features involved in *Bacillus subtilis* biofilm formation using multi-culturing approaches. *Microorganisms* 2021;9:633.
- [49] Priestler JH, Horst AM, Van De Werfhorst LC, Saleta JL, Mertes LAK, Holden PA. Enhanced visualization of microbial biofilms by staining and environmental scanning electron microscopy. *J Microbiol Methods* 2007;68:577–87.
- [50] Bossù M, Selan L, Artini M, Relucenti M, Familiari G, Papa R, Vrenna G, Spigaglia P, Barbanti F, Salucci A, Di Giorgio G, Rau JV, Polimeni A. Characterization of *Scardovia wiggsiae* Biofilm by original scanning electron microscopy protocol. *Microorganisms* 2020;8:807.
- [51] Gingichashvili S, Duanis-Assaf D, Shemesh M, Featherstone JDB, Feuerstein O, Steinberg D. The adaptive morphology of *Bacillus subtilis* biofilms: a defense mechanism against bacterial starvation. *Microorganisms* 2019;8:62.
- [52] Asally M, Kittisopikul M, Rué P, Du Y, Hu Z, Çağatay T, Robinson AB, Lu H, Garcia-Ojalvo J, Süel GM. Localized cell death focuses mechanical forces during 3D patterning in a biofilm. *Proc Natl Acad Sci U S A* 2012;109:18891–6.
- [53] Shemesh M, Chai Y. A combination of glycerol and manganese promotes biofilm formation in *Bacillus subtilis* via Histidine Kinase KinD Signaling. *J Bacteriol* 2013;195:2747–54.
- [54] Oppenheimer-Shaanan Y, Sibony-Nevo O, Bloom-Ackermann Z, Suissa R, Steinberg N, Kartvelishvily E, Brumfeld V, Kolodkin-Gal I. Spatio-temporal assembly of functional mineral scaffolds within microbial biofilms. *npj Biofilms Microbiome* 2016;2:15031.
- [55] Arabolaza AL, Nakamura A, Pedrido ME, Martelotto L, Orsaria L, Grau RR. Characterization of a novel inhibitory feedback of the anti-anti-sigma SpoIIAA on Spo0A activation during development in *Bacillus subtilis*. *Mol Microbiol* 2003;47:1251–63.
- [56] Wang X, Meng S, Han J. Morphologies and phenotypes in *Bacillus subtilis* biofilms. *J Microbiol* 2017;55:619–27.
- [57] Magan N, Lacey J. Effect of water activity and temperature on mycotoxin production by *Alternaria alternata* in culture and wheat grain. *Appl Environ Microbiol* 1984;47:1113–7.
- [58] O'Toole G, Kaplan HB, Kolter R. Biofilm formation as microbial development. *Annu Rev Microbiol* 2000;54:49.
- [59] Yu SM, Lee YH. Effect of light quality on *Bacillus amyloliquefaciens* JBC36 and its biocontrol efficacy. *Biol Control* 2013;64:203–10.
- [60] Ostrov I, Sela N, Belausov E, Steinberg D, Shemesh M. Adaptation of *Bacillus* species to dairy associated environment facilitates their biofilm forming ability. *Food Microbiol* 2019;82:316–24.
- [61] Julkowska D, Obuchowski M, Holland IB, Séror SJ. Comparative analysis of the development of swarming communities of *Bacillus subtilis* 168 and a natural wild type: critical effects of surfactin and the composition of the Medium. *J Bacteriol* 2005;187:65–76.
- [62] Abee T, Kovács ÁT, Kuipers OP, van der Veen S. Biofilm formation and dispersal in Gram-positive bacteria. *Curr Opin Biotechnol* 2011;22(2):172–9.
- [63] Kobayashi K. *Bacillus subtilis* pellicle formation proceeds through genetically defined morphological changes. *J Bacteriol* 2007;189:4920–31.
- [64] Vlamakis H, Aguilar C, Losick R, Kolter R. Control of cell fate by the formation of an architecturally complex bacterial community. *Chemtracts* 2007;22(7):945–53.

- [65] Bais HP, Fall R, Vivanco JM. Biocontrol of *Bacillus subtilis* against infection of *Arabidopsis* roots by *Pseudomonas syringae* is facilitated by biofilm formation and surfactin production. *Plant Physiol* 2004;134:307–19.
- [66] Chen Y, Yan F, Chai Y, Liu H, Kolter R, Losick R, Guo JH. Biocontrol of tomato wilt disease by *Bacillus subtilis* isolates from natural environments depends on conserved genes mediating biofilm formation. *Environ Microbiol* 2013;15:848–64.
- [67] Pandin C, Darsonval M, Mayeur C, Le Coq D, Aymerich S, Briandeta R. Biofilm formation and synthesis of antimicrobial compounds by the biocontrol agent *Bacillus velezensis* QST713 in an *Agaricus bisporus* compost micromodel. *Appl Environ Microbiol* 2019;85:1–13.
- [68] Nagórska K, Bikowski M, Obuchowski M. Multicellular behaviour and production of a wide variety of toxic substances support usage of *Bacillus subtilis* as a powerful biocontrol agent. *Acta Biochim Pol* 2007;54:495–508.
- [69] Jeyaram K, Romi W, Singh TA, Adewumi GA, Basanti K, Oguntoyinbo FA. Distinct differentiation of closely related species of *Bacillus subtilis* group with industrial importance. *J Microbiol Methods* 2011;87:161–4.
- [70] Gómez J, Luisa Gómez-Lus M, Bas P, Ramos C, Cafini F, Maestre JR, Prieto J. Biofilm score: is it a differential element within gram negative bacilli? *Rev Española Quimioter* 2013;26(2):97–102.
- [71] Liu J, W M, Droby S, Tian S, Hershkovitz V, Tworowski T. Effect of heat shock treatment on stress tolerance and biocontrol efficacy *Metschnikowia fructicola*. *FEMS Microbiol Ecol* 2011;76:145–55.
- [72] Rabbee M, Ali M, Choi J, Hwang B, Jeong S, Baek K. *Bacillus velezensis*: a valuable member of bioactive molecules within plant microbiomes. *Molecules* 2019;24:1046.